Rev. Adv. Mater. Tech. vol. 3 no 3 (2021) 1-9
DOI:10.17586/2687-0568-2021-3-3-1-9

IDENTIFICATION OF ACOUSTIC EMISSION SOURCES IN A POLYMER COMPOSITE MATERIAL UNDER CYCLE TENSION LOADING

A.A. Bryansky, O.V. Bashkov and A.E. Protsenko

Department of materials science and technology of new materials, Komsomolsk-na-Amure State University, Lenin street, 27, Komsomolsk-on-Amur, 681013, Russia

Received: September 20, 2021

Abstract. The paper is devoted to identification damages which developing in the polymer composite material (PCM) structure during fatigue tests, based on the frequency components of the recorded acoustic emission (AE) signals. The objects of the study were specimens made of DION 9300 FR binder and 46 layers of T11-GVS9 fiberglass fabric. Mechanical tests were cyclic tension with AE recording. Fourier spectra for AE signals were calculated and used for the self-organizing Kohonen map (SOM) at the first stage of clustering. At the second stage, a k-means algorithm was used to find clusters with similar centroids and combine them. For the clusters obtained, their nature was determined from the peak frequencies and the periods of their critical accumulation were calculated. Additionally, the peak frequencies analysis of the wavelet decomposition levels was done.

1. INTRODUCTION

Analysis of acoustic emission (AE) generated by a polymer composite material (PCM) under loading is often a non-trivial task. The complex structure of the filler and interfacial interactions with the matrix characterize the formation in the material of various types of damage, their sequence and combinations, which affects the recorded and calculated parameters.

Many fracture models of laminated plastics are based on static tension or bending and can be used to determine the dominant types of damage and their classification by AE parameters. However, when it is difficult to estimate the fracture processes in advance, as in the case of mechanical fatigue loading, algorithms for clustering AE parameters have found application.

The most commonly used parameters to describe the recorded AE are the amplitude, rise time and duration of the signal, energy, median and peak frequencies [1-3]. In [4], the efficiency of polymer composite damage identification by the peak frequency of the recorded AE signals is shown, which is confirmed by the results of microscopic studies. But it is more efficient to analyze several parameters at once, which avoids the limitations of each parameter taken separately. For example, in [5], the identification of fiberglass damage clusters with the separation of the matrix damage types done by amplitudes and duration distribution of AE signals.

In [6], the most effective parameters of the AE signals for analysis were selected by the Laplacian score. High values of the Laplacian score, indicating a high representativeness of the data, were obtained for the peak amplitude, peak and median frequencies. Thus, it can be concluded that waveform or frequency representation of the signals is a set of AE parameters that allow identify structural changes and their features with high accuracy [7-9].

To characterize AE signals, the parameters of the wavelet decomposition levels can also be used [2,10]. Earlier, the authors [11] tested the analysis technique based on the Daubechies wavelet of the 14th order for 7 levels of decomposition of AE signals. The technique

Corresponding author: A.A. Bryansky, e-mail: bryansky.aa@yandex.ru

consisted in associating a certain type of damage to each decomposition level in accordance with its frequency range. Classification was made based on the analysis of peak frequencies characterizing different types of damage. This technique was tested in the analysis of AE signals recorded at three-point static bending of fiberglass samples.

One of the effective methods of statistical analysis of AE is data clustering. In the absence of characterizing information about the parameters, unsupervised methods are used. These include the k-means algorithm [2] and the self-organizing map (SOM) [12-14]. In works [6,13,14], the methods of analysis of amplitudes and frequency components of AE signals were successfully applied for the clustering problem. In [15], for signal clustering, the authors used energy and peak frequencies parameters.

Many researchers note the possibility of using the frequency representation of signals as a set of characteristics of various types of damage. However, only a few parameters are selected from the frequency representation of signals, such as peak and median frequencies [16], although clustering algorithms allow the use of multiparameter data.

The aim of the study is to identify damages arising in the structure of a PCM during cyclic loading.

2. MATERIALS AND METHODS

The object of the study was dog-bone samples, cut from a fiberglass plate, with a rectangular section of 10 × 10 mm (Fig.1a). The plate was made by vacuum infusion using DION 9300 FR epoxy vinyl ester binder and 46 layers of T11-GVS9 glass fabric.

Mechanical tests were carried out on a servo-hydraulic testing machine using the cyclic stretching method (Fig. 1b). The load value was chosen equal to half of the breaking load and amounted to 300 MPa.

Microscopic studies of the specimens were carried out on a Hitachi SEM S-3400N scanning electron microscope. The tested specimens were sawn according to Fig. 1c for three surfaces to examine. Analysis of the microstructure in planes near and far from the specimen rupture makes it possible to evaluate cracks at different depths. Also the difference in the cross-sectional areas of the specimens in the dog-bone form provides the material stress gradient, which allows obtaining more information about the developed damage.

AE registration was carried out on the AE 2.1 Pro hardware-software complex using a GT301 wideband sensor (50–550 kHz). The processing of the recorded AE signals was carried out according to the scheme shown in Fig. 2 in the MATLAB environment.

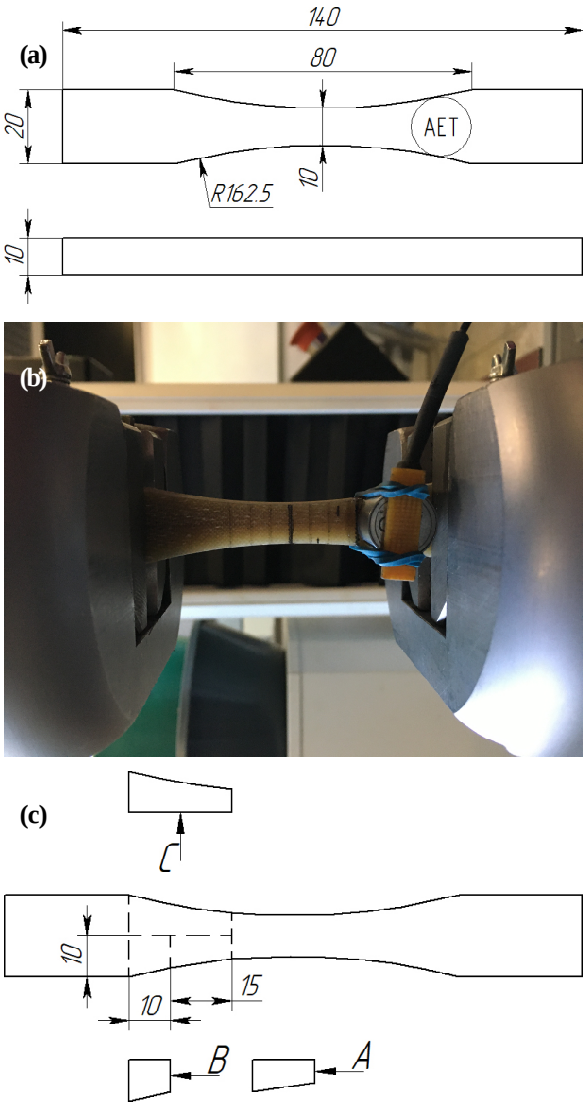

Fig. 1. Pictures of specimens: (a) geometry and dimensions of the specimen, (b) specimen in test, (b) location of planes for microscopic examinations.

AE data clustering was implemented in two stages: clustering with a self-organizing Kohonen map and subsequent clustering of the obtained centroids using the k-means algorithm. For the recorded AE signals, the Fourier spectra were calculated, from which only the informative part (24–450 kHz), containing characteristic information about the destruction processes in the PCM [6,17,18] was taken and normalized. The limitation of the spectrum analyzed part reduces the influence of noise which presented by very low and very high frequencies [12], normalization of the spectra reduces the influence of the signal amplitude [15]. The obtained spectra were input to a self-organizing map. The number of output clusters (equal to 100 pieces) was selected empirically based on the reproducibility of clustering results, including for other types of mechanical tests [19]. Such

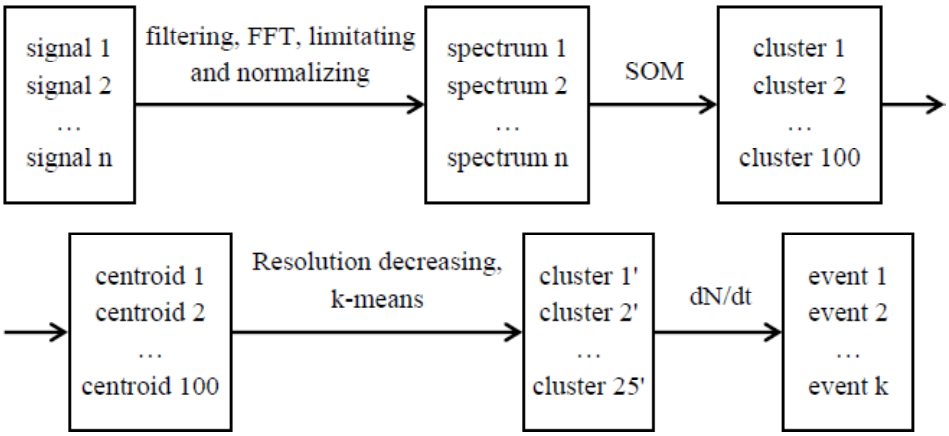

Fig. 2. Scheme for the recorded AE signals processing.

number of clusters makes it possible to separate AE signals from formed damages of a mixed nature in the material and noise signals separately [12].

Further, the clusters were combined according to their centroids similarity. The small amount of data (100 centroids) and a large number of their parameters (1352 points) lead to unsatisfactory clustering results [7]. Reducing the dimension of the data, and in this case, reducing the resolution of the spectra (centroids), makes it possible to increase the efficiency of using k-means and other algorithms [15]. The centroid resolution was lowered with averaging method to a step of 5 kHz (86 points in total). With the number of possible damage types and their combinations, the number of output clusters was taken equal to 25. The clusters were combined with the condition that the centroid of the largest cluster of the first stage within the cluster of the second stage was taken to characterize the cluster of the second stage.

The analysis of the accumulation curves of each AE signals cluster was done according to the change of their accumulation intensity. Active development of a certain type of damage, and not only registration of its formation, presents great information value. Taking into account that the process of active development of a defect is characterized by a cyclic registration of AE events [20] and a nonlinear nature of damage accumulation in materials with a complex structure [21], the AE activity value equal to 2 s^{-1} was taken as the threshold for the formation activity of a certain type of damage.

The scale of damage formation in the material (local or global) was estimated from the spread of the peak frequencies of each decomposition level. Spread of the peak frequency values of each level makes it possible to estimate the scale (local or global) of the damage in the volume of the material, on the basis of influence of the propagation path length of the acoustic wave from the damage to the AE transducer on the peak frequency of the signal [2]. For the analysis, the median values and the values of the standard deviation of the peak frequencies were selected. Median value of the peak amplitude was used to determine the prevailing type of damage to the PCM or its scale, and the volume of formed damage was estimated from the standard deviation of the values. The stage limits were taken from the analysis of the clusters accumulation.

3. RESULTS

3.1. Two stage clustering SOM and k-means

As a result of the AE signals processing according to the scheme shown in Fig. 2, 18 clusters were obtained. The characterization of clusters matching to specific types of damage was done by the values of the peak frequencies. In [2,6,7] found that frequencies of 30–150 kHz indicate to matrix microdamages, frequencies 130–220 kHz indicate to the formation of delamination, and frequencies 230–310 kHz, 180–290 kHz and over 380 kHz indicate to debonding, slipping and breaking of glass fibers, respectively. In this study, in the frequency range characterizing microdamage to the matrix, 4 peaks were confirmed: 25–40, 55–70, 80, and 100–105 kHz.

During three-point bend test of the specimens made of only binder at the moment of sliding of specimen over the supports, AE signals with a peak frequency of about 68 kHz were recorded. During tensile test of the specimen at the moment of insertion of the clamps of the testing machine into the surface of the binder and its damage, AE signals with peak frequencies of 27 and 67 kHz were recorded. When three-point bend testing PCM, matrix damages are characterized by a peak frequency range of 24–110 kHz. Based on these data, it was assumed that frequencies of 30–70 and 80 kHz characterize matrix damage of scales 1 and 2 (shear and compression microdamages), 100 kHz characterize matrix

Table 1. Characteristics of the damage types by frequency.

Frequencies, kHz	Type of damage
30–70, 80 and 100	Matrix damages of scale 1, 2 and 3 respectively
130–150	Critical matrix damage (interlayer damage)
150–220	Delamination
180–260	Fibers slipping
270–310	Fibers debonding
360–400	Fibers failure

damage of scale 3 (chips, breaks), and 130–150 kHz indicate delamination damage. The correspondence of peak frequencies to the types of formed damages adopted in this work is given in Table 1.

Table 2 shows the peak frequencies of the obtained clusters of the AE signals spectra. Addition of the mixed damage cluster can partially solve the problem of high activity AE, resulting in various damages of registration in the form of one long acoustic signal [12].

Solving the problem of determining the destruction process stages, the sequence and compatibility of the resulting defects is important. Therefore, for each cluster, the periods were determined in which the intensity

Table 2. Characteristics of the clusters by peak frequencies.

№	Frequencies, kHz	Description
RC1	35, 100, 380–400 (low 60 and 80)	Matrix and fibers combined damage
RC2	370–400	Fibers failure
RC3	35–400	Mixed types damage
RC4	35	Matrix damage of scale 1
RC5	170–260, 300, 360–400 (low 35–130)	Debonding, slipping and fibers failure
RC6	300–310, 360–380 (low 240–250)	Debonding and fibers failure
RC7	30, 80 (low 60 and 100)	Matrix damage, scales 1 and 2 prevail
RC8	30–60 (low 80–100)	Matrix damage, scale 1 prevails
RC9	100	Matrix damage of scale 3
RC10	60–80	Matrix damage of scale 2
RC11	100 (low 30–80)	Matrix damage, scale 3 prevails
RC12	60–80, 380 (low 30 and 100)	Matrix of scale 2 and fibers combined damage
RC13	200–240 (low 270–300 and 360–400)	Delamination forming, fibers failure
RC14	170–180, 360–380	Slipping and fibers failure
RC15	80	Matrix damage of scale 2
RC16	180 (low 30–130 and 380)	Interlayer damage (delamination)
RC17	30, 80–130, 150	Critical matrix damage
RC18	100, 360–380	Matrix scale of 3 and fibers combined damage

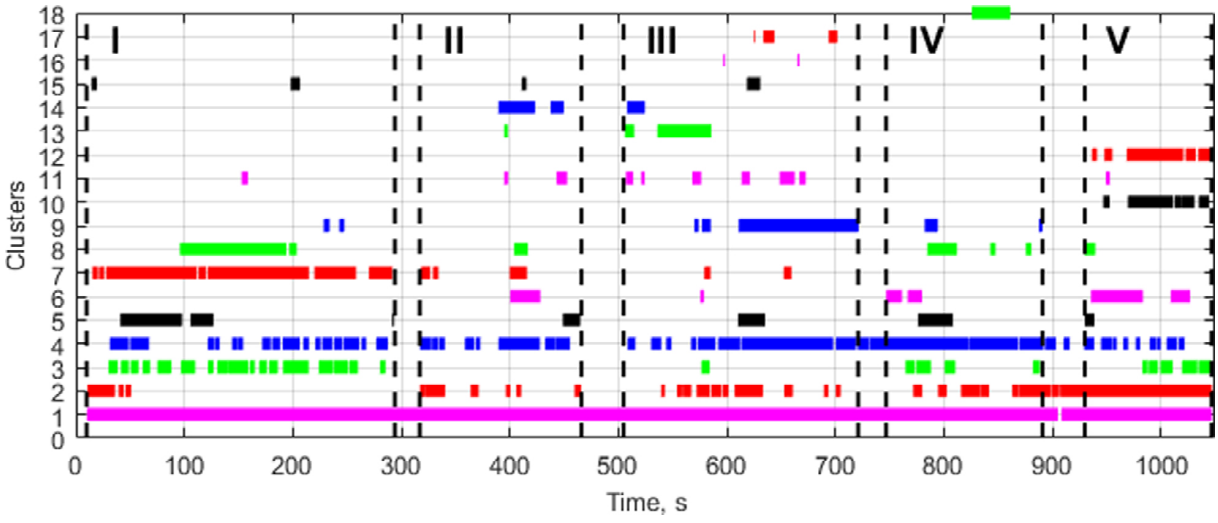

Fig. 3. Exceeding the threshold intensity of accumulation of each type clusters during testing.

Table 3. Frequency ranges of decomposition levels.

Decomposition level	Frequency range, kHz	Damage type
1	1250–2500	-
2	625–1250	-
3	312,5–625	Fibers failure
4	156,25–312,5	Adhesion loss (delamination, fibers debonding)
5	78,13–156,25	Critical matrix damage
6	39,06–78,13	Matrix macrodamage
7	19,53–39,06	Matrix microdamage

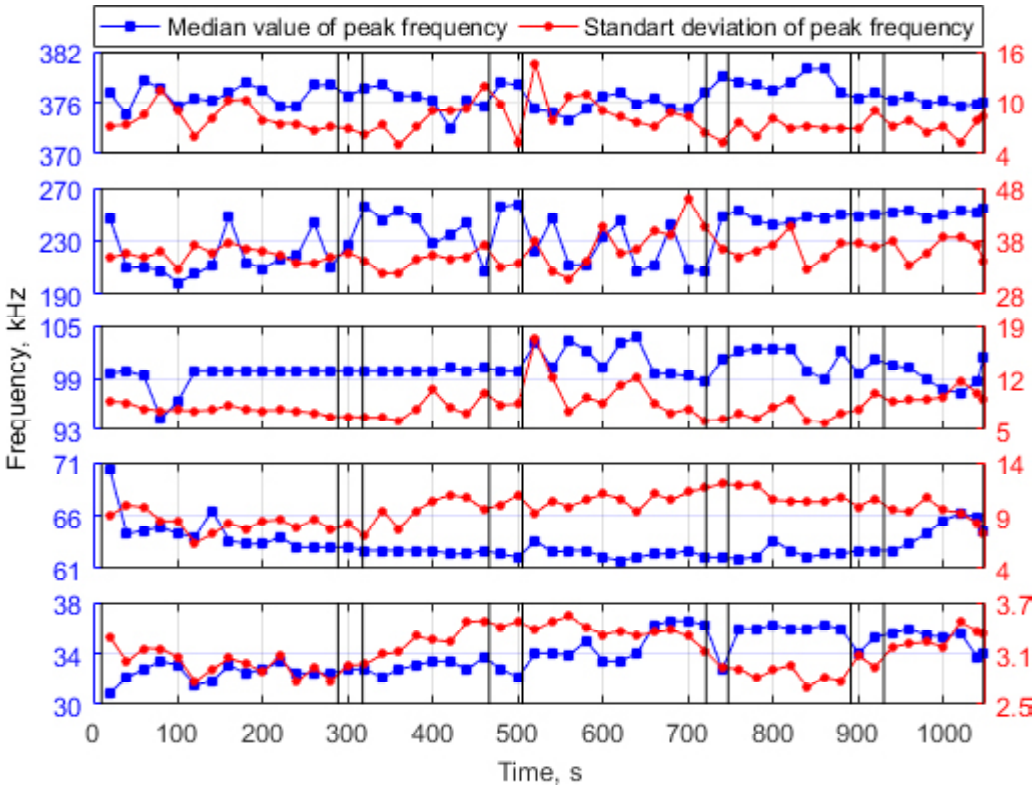

Fig. 4. – Change in the median value of the peak frequencies and their standard deviations for decomposition levels from 3 to 7 (from top to bottom).

of registration of each damage type events exceeds the threshold of AE activity, equal to 2 s^{-1}. The periods of active accumulation of each cluster are shown in Fig.3.

First of all, the periods of damage only to the matrix of scale 1 and glass fibers were taken as the boundaries of the stages. As a result, 5 stages were identified. All stages of material destruction can be characterized by the permanent formation of combined damage to the matrix with fibers and separate damage to the matrix. In addition, the accumulation of damage to only glass fibers, which becomes more intense from stage to stage, stands out separately.

Stage I. Mostly characterized by the matrix damage on a scale of no more than 2. Fibers damage is most likely caused by damage to the specimen in the grips of the testing machine at the beginning of the stage.

Stage II. Combined matrix and fibers damage is formed. An interlayer crack is initiated, which results in scale 3 matrix damage as well as more complex and intense fiber damages.

Stage III. The formation of combined matrix and fibers damage continue; the growth of interlayer cracks. From the middle of the stage, periodic critical damage to the matrix registered, the intensity of the formation of damage to the matrix of scale 3 increases significantly.

Stage IV. The process of combined matrix and fibers damages formation becomes more uniform and is accompanied by periodic registration of mixed damages of

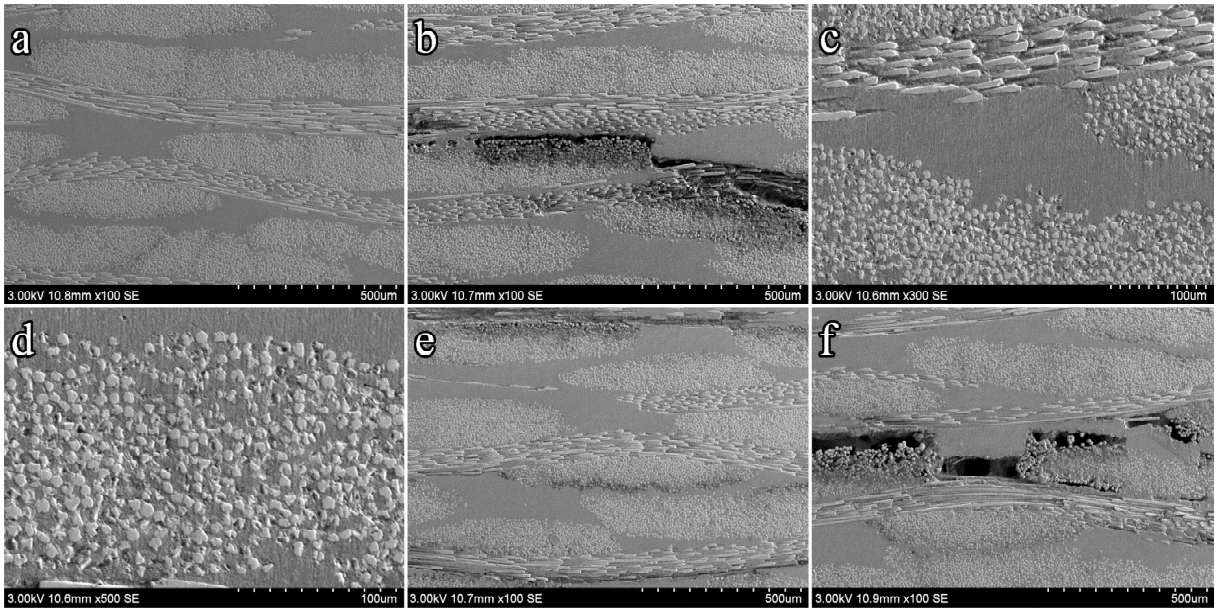

Fig. 5. Plane A microscopy: (a-d) surface layers, (e-f) inner layers.

the material. The matrix damage is represented by scale 1, and the mechanism of fiber damage is mainly represented only by fracture of the fibers.

Stage V. The scale of matrix damage in the combined formation of damage with fibers increases to a scale of 2. Mixed damage to the material and matrix damage of scales 1 and 2 with a predominance of scale 2 are formed.

3.2. Wavelet-decomposition

Table 3 shows the frequency ranges calculated by the levels of the wavelet decomposition, with the corresponding types of damage established to them. The analysis was performed using the median values and the values of the standard deviation of the peak frequencies (Fig. 4).

At the first stage of the material destruction, the matrix damage of scale 1 and larger damage occurs locally with a tendency to reduce the scale of the resulting damage. Damage associated with glass fibers is mainly represented by adhesion loss to the binder.

The scale of matrix damage at the second stage begins to take on a global character. The intensity of the fibers debonding decreases, and their fracture begins in the volume of the material.

At the third stage, matrix damage occurs locally, but with an increase in their scale (in the center of the sample). Fracture of the fibers again acquires a local character, and damage of the adhesion loss type is formed chaotically.

At the fourth stage, matrix damage occurs locally and damage scale continues to growth. Active global debonding and slipping of fibers with their subsequent fracture.

The fifth stage is characterized by global critical damage to the material and destruction of the specimens.

3.3. Microscopy

As a result of microscopic studies, images of the structures presented at Figs. 5-7 were obtained.

In the surface layers in the plane A, delamination is observed passing at the boundary of the warp fibers bundles with a damage of the bundle structure (Fig. 5). Intralayer damages are in the fiber bundles of the fabric warp, a small part of the fibers debond and slipped out (Fig. 10a). At higher magnification, the fibers slipping found which is characteristic of stretching (figs. 5c and 5d).

In the central part of plane A, the scale of the interlayer crack is larger, however, the crack itself is located between the bundles of warp and weft fibers (Fig. 5f). The debonds of the fibers of the fiberglass warp has a more concentrated distribution (Fig. 5e).

In the surface layers of the plane B, debonds fibers of the fiberglass warp observed too, but their number is less (Fig. 6a). Interlayer cracks affect the fiber bundles less and are characterized at their boundary. Thus a greater extent of damage observed in bundles of fiberglass weft fibers (Figs. 6b-6d).

With distance from the specimen failure in plane C in the surface layers, the damages of the weft fibers acquire a more distributed character with a decrease in their number (Figs. 7a-7d). In the central part of the plane C, an interlayer crack is characterized at the border of the fiberglass weft bundles and matrix. With distance from the failure site, the crack width decreases, and the damage is distributed in the structure of the fiberglass

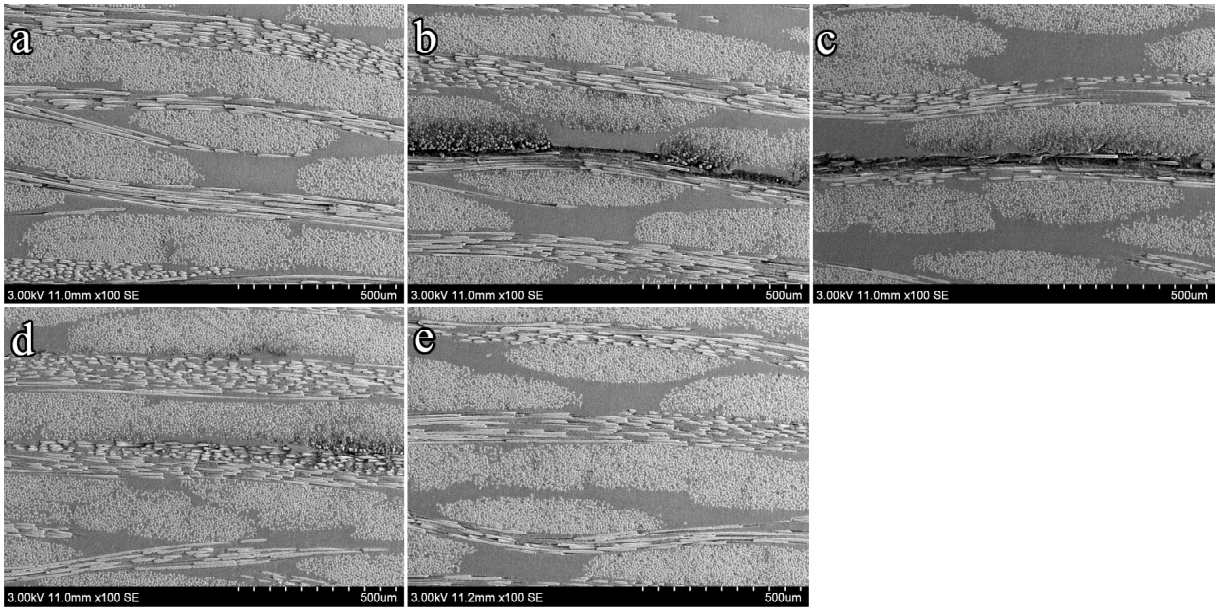

Fig. 6. Plane B microscopy: (a-d) surface layers, (e) inner layers.

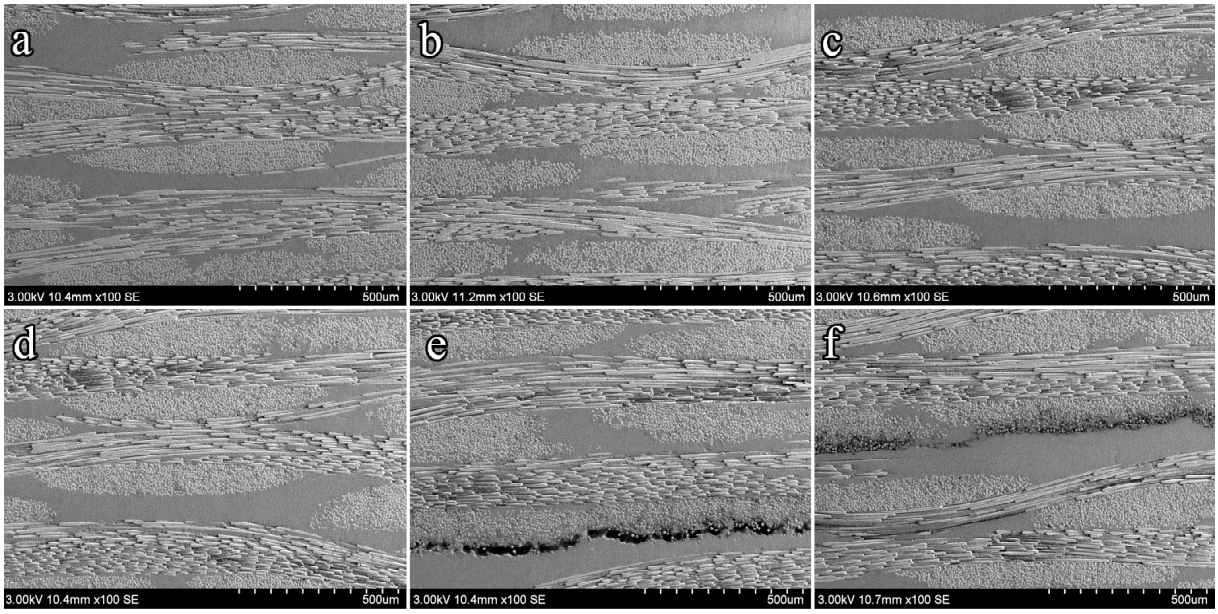

Fig. 7. Plane C microscopy: (a, c) surface layers closer to failure site, (b-d) surface layers with distance to failure site, (e) inner layers closer to failure site, (f) inner layers with distance to failure site.

weft bundles. Damage to the fibers of the warp fabric retains a similar appearance with distance from the failure site (Fig. 7e and 7f).

4. DISCUSSION

In [22], the process of destruction of a CFRP specimen under static tension was studied using an acoustic pulse microscope. The onset of destruction was registered by the formation of matrix microdamages along the fibers and their debonding. The destruction process continues with the accumulation of damage inside the layers with the development of macroscopic damage - delamination, up to the rupture of the specimen. In [2], a similar fracture characteristic of CFRP under static tension was obtained. Accordingly, it was concluded that the process of damage accumulation during cyclic and static tension has a similar nature and sequence, which is also noted in work [23]. In many studies, mechanical tests are performed in accordance with accepted standards, while during the operation of PCM products, loads with different values of force and vector of their application are possible. Therefore, further studies of PCMs under cyclic loading conditions with different load levels are important.

The stages of destruction obtained in [22] is comparable to that obtained in this work, however, stage I,

which precedes the fiber adhesion loss to the binder matrix, allows one to register the onset of microscopic destruction of the material. A similar result - separated registration of damage to glass fibers at the initial stages of loading - was obtained for PCM filled with short fibers [1]. Thus, it is possible not only to single out the processes leading to a decrease in the bearing capacity of PCM, but also to register the previous processes of damage formation.

Comparing the results of the wavelet decomposition analysis of AE signals of this work and the results of a study using a similar method [24], information on the statistic distribution of the of the wavelet decomposition level parameters can be used to assess the scale of damage and their distribution in the volume of the material. Despite the obtained result, this technique needs additional research with other types of PCM and testing method.

Comparing the microscopic examination results of the specimen with the analysis results of the registered AE parameters, similar information about the resulting damage formed. The registered damage by the AE parameters, characterized as a matrix and fibers combined damage, is formed at the matrix/fiber interface and is presented as cleavage of the matrix or fibers. When a certain critical amount of this locally generated damage is reached, the fiber bundles are disrupted and their contact with the matrix is lost. If the scale of the matrix is large in matrix and fibers combined damage, these damages lead to the formation of interlayer cracks.

At a distance from the failure site, in the zone of lower stresses, microdamages are located globally. Closer to the failure site, the scale of damage is larger, and large damage is located in the center of microdamage. At stage IV, clusters of critical interlayer damage were identified, also detected during microscopic examination of the sample, characterizing critical damage to the composite structure and its final destruction at stage V.

5. CONCLUSION

On the basis of two analyzing methods for the AE data, the types of fracture were identified and the stages of damage accumulation in PCM specimens under cyclic loading were identified.

The initiation of the PCM destruction begins with matrix damage, leading to a loss of adhesion both between the binder and the fibers, and between the layers of the PCM. Defectioning of the material structure turns into a chaotic process, ending with a fracture of the main part of the fibers and large-scale damage to the matrix up to failure.

It has been found that by the local formation of matrix microdamages and the fracture of a part of the fibers, it is possible to identify and prevent the destruction of the material, and by registering damage by the type of loss of adhesion, it is possible to identify the beginning of the material destruction

ACKNOWLEDGEMENTS

The reported study was funded by Russian science foundation, project number 21-19-00896.

REFERENCES

[1] F. Willems, J. Benz and C. Bonten, *Detecting the critical strain of fiber reinforced plastics by means of acoustic emission analysis*, Journal of Acoustic Emission, 2016, vol. 33, pp. 525–534. https://www.ndt.net/article/ewgae2016/papers/525_paper.pdf

[2] R. Gutkin, C.J. Green, S. Vangrattanachai, S.T. Pinho, P. Robinson and P.T. Curtis, *On acoustic emission for failure investigation in CFRP: Pattern recognition and peak frequency analyses*, Mechanical systems and signal processing, 2011, vol. 24, no. 10, pp. 1393-1407. https://doi.org/10.1016/j.ymssp.2010.11.014

[3] A.I. Shilova, V.E. Vildeman, D.S. Lobanov and Yu.B. Lyamin, *Researching mechanisms of carbon composites fracture based on the mechanical tests monitoring acoustic emission*, PNRPU Mechanics Bulletin, 2013, vol. 2, pp. 169-179. https://doi.org/10.15593/perm.mech/2013.4.169-179

[4] M. Nikbakht, J. Yousefi, H. Hosseini-Toudeshky and G. Minak, *Delamination evaluation of composite laminates with different interface fiber orientations using acoustic emission features and micro visualization*, Composites Part B: Engineering, 2017, vol. 113, pp. 185-196. https://doi.org/10.1016/j.compositesb.2016.11.047

[5] Y. Ech-Choudany, M. Assarar, D. Scida, F. Morain-Nicolier and B. Bellach, *Unsupervised clustering for building a learning database of acoustic emission signals to identify damage mechanisms in unidirectional laminates*, Applied Acoustics, 2017, vol. 123, pp. 123-132. https://doi.org/10.1016/j.apacoust.2017.03.008

[6] L. Li, S.V. Lomov, X. Yan and V. Carvelli, *Cluster analysis of acoustic emission signals for 2D and 3D woven glass/epoxy composites*, Composite Structures, 2014, vol. 116, pp. 286-299. https://doi.org/10.1016/j.compstruct.2014.05.023

[7] M.G.R. Sause, *Acoustic emission source identification in large scale fibre reinforced composites*, Journal of Acoustic Emission, 2016, vol. 33, pp. 441-450. https://www.ndt.net/article/ewgae2016/papers/441_paper.pdf

[8] V.I. Ivanov, P.A. Belov and T.S. Nasibullin, *Defects in composite materials as sources of acousticissue*, Znanie, 2016, vol. 3, no. 2, pp. 23-29.

[9] R. De Oliveira and A.T. Marques, *Health monitoring of FRP using acoustic emission and artificial neural networks*, Computers & structures, 2008, vol. 86, no. 3-5, pp. 367-373. https://doi.org/10.1016/j.compstruc.2007.02.015

[10] G. Qi, A. Barhorst, J. Hashemi and G. Kamala, *Discrete wavelet decomposition of acoustic emission signals from carbon-fiber-reinforced composites*, Composites Science and Technology, 1997, vol. 57, no. 4, pp. 389-403. https://doi.org/10.1016/S0266-3538(96)00157-1

[11] A.A. Bryansky, O.V. Bashkov, I.O. Bashkov and D.B. Solovev, *PCM bearing capacity prediction criteria development based on registered AE parameters*, IOP Conference Series: Earth and Environmental Science, 2020, vol. 459, no. 6, art. 062105. https://doi.org/10.1088/1755-1315/459/6/062105

[12] E.v.K. Hill, C.J. Foti, N.Y. Leung and A.E. Palacios, *Neural network burst pressure prediction in tall graphite-epoxy pressure vessels from acoustic emission data*, Journal of Acoustic Emission, 2012, vol. 33, pp. 167-180. https://www.ndt.net/article/jae/papers/30-167.pdf

[13] L. Li, S.V. Lomov and X. Yan, *Correlation of acoustic emission with optically observed damage in a glass/epoxy woven laminate under tensile loading*, Composite structures, 2015, vol. 123, pp. 45-53. https://doi.org/10.1016/j.compstruct.2014.12.029

[14] D. Xu, P.F. Liu, Z.P. Chen, J.X. Leng and L. Jiao, *Achieving robust damage mode identification of adhesive composite joints for wind turbine blade using acoustic emission and machine learning*, Composite Structures, 2020, vol. 236, art. 111840. https://doi.org/10.1016/j.compstruct.2019.111840

[15] M. Enoki, Y. Muto and T. Shiraiwa, *Evaluation of deformation behavior in LPSO-magnesium alloys by AE clustering and inverse analysis*, Journal of Acoustic Emission, 2016, vol. 33, pp. 145-150.

[16] T. Bohmann, M. Schlamp and I. Ehrlich, *Acoustic emission of material damages in glass fibre-reinforced plastics*, Composites Part B-Engineering, 2018, vol. 155, pp. 444-451. https://doi.org/10.1016/j.compositesb.2018.09.018

[17] Z. Hamam, N. Godin, C. Fusco and T. Monnier, *Modelling of fiber break as Acoustic Emission Source in Single Fiber Fragmentation Test: comparison with experimental results*, Journal of Acoustic Emission, 2018, vol. 35, pp. 1-12. https://www.ndt.net/article/ewgae2018/papers/6.pdf

[18] M.G.R. Sause, *On use of signal features for acoustic emission source identification in fibre-reinforced composites*, Journal of Acoustic Emission, 2018, vol. 35, pp. 1-12. https://d-nb.info/1212797426/34

[19] A.A. Bryansky, O.V. Bashkov, D.P. Malysheva and D.B. Solovev, *Investigation of the Staging of Damage Accumulation in Polymer Composite Materials during Bending and Tensile Tests*, Key Engineering Materials, 2021, vol. 887, pp. 116-122. https://doi.org/10.4028/www.scientific.net/KEM.887.116

[20] D.V. Chernov, V.M. Matyunin, V.A. Barat, A.Y. Marchenkov and S.V. Elizarov, *Investigation of acoustic emission in low-carbon steels during development of fatigue cracks*, Russian Journal of Nondestructive Testing, 2018, vol. 54, no. 9, pp. 638-647. https://doi.org/10.1134/S1061830918090024

[21] V.V. Bardakov, A.I. Sagaydak and S.V. Elizarov, *Acoustic emission behaviour of over-reinforced concrete beams*, Kontrol. Diagnostika, 2019, vol. 9, pp. 4-12. https://doi.org/10.14489/td.2020.06.pp.032-039

[22] Y.S. Petronyuk, V.M. Levin, E.S. Morokov, T.B. Ryzhova, A.V. Chernov and I.V. Gulevsky, *Studying the dynamics of microdefect growth in carbon fiber reinforced plastics under mechanical loading by means of ultrasonic microscopy*, Bulletin of the Russian Academy of Sciences: Physics, 2016, vol. 80, no. 10, pp. 1224-1228. https://doi.org/10.7868/S0367676516100185

[23] W. Roundi, A. El Mahi, A. El Gharad and J.L. Rebiere, *Acoustic emission monitoring of damage progression in glass/epoxy composites during static and fatigue tensile tests*, Applied Acoustics,2018, vol. 132, pp. 124-134. https://doi.org/10.1016/j.apacoust.2017.11.017

[24] C.S. Kumar, V. Arumugam, S. Sajith, H.N. Dhakal and R. John, *Acoustic emission characterisation of failure modes in hemp/epoxy and glass/epoxy composite laminates*, Journal of Nondestructive Evaluation, 2015, vol. 34, no. 4, art. 31. https://doi.org/10.1007/s10921-015-0306-8